Research Article

Wafa M. Al-Saleh, Mai R. H. Dahi, M. I. Sayyed, Haifa M. Almutairi, I. H. Saleh, and Mohamed Elsafi*

Comprehensive study of the radiation shielding feature of polyester polymers impregnated with iron filings

https://doi.org/10.1515/epoly-2023-0096
received July 09, 2023; accepted August 07, 2023

Abstract: Radiation and nuclear technologies have side effects in addition to their important applications, so appropriate shields must be used to protect users and the public from high doses as a result of exposure to this radiation. In this work, the attenuation coefficients for polyester composites doped with waste iron filings (IFs) were studied. Six samples of different IF concentrations were manufactured, namely, Poly, Poly-IF20, Poly-IF30, Poly-IF40, Poly-IF50, and Poly-IF60 (where Poly-IF60 represents 40% polyester and 60% IF). We measured the attenuation factors using high purity germanium (HPGe)-detector along with three radioactive sources ^{241}Am (emitting energy of 0.06 MeV), ^{137}Cs (emitting energy of 0.662 MeV), and Co-60 (emitting energy of 1.173 and 1.333 MeV). We compared the linear attenuation coefficient (LAC) obtained by theoretical (i.e., XCOM software) and experimental (i.e., HPGe-detector) approaches for the prepared polyester composites at various photon energies (0.060, 0.662, 1.173, and 1.333 MeV). The greatest difference between the LAC values of the samples occurs at 0.060 MeV, where the Poly-IF60 sample has a much greater LAC than the other shields, followed by the Poly-IF50 sample, Poly-IF40 sample, and so on until the pure polyester shield. Specifically, their values are equal to 0.245, 0.622, 0.873, 1.187, 1.591, and 2.129 cm^{-1} for Poly, Poly-IF20, Poly-IF30, Poly-IF40, Poly-IF50, and Poly-IF60, respectively. We calculated the transmission factor (TF) and the radiation shielding efficiency (RSE), and found that the TF for Poly-IF30 is equal to 28.82%, 77.94%, 82.75%, and 83.75% at 0.060, 0.662, 1.173, and 1.333, respectively, while its RSE is equal to 82.57%, 24.00%, 18.80%, and 17.72%, respectively. The fast neutron removal cross-section (FNRC) of the polyester samples was calculated and the values increase when more Ifs are added to the samples. More specifically, the FNRC values are equal to 0.095, 0.100, 0.103, 0.107, 0.110, and 0.113 cm^{-1} for Poly, Poly-IF20, Poly-IF30, Poly-IF40, Poly-IF50, and Poly-IF60, respectively.

Keywords: polyester, iron filings, shielding, gamma-rays, neutrons

1 Introduction

Shielding is considered one of the most important requirements for radiation protection along with the duration of exposure and the distance between the person and the radiation source. Radiation shielding is necessary in medical and industrial places such as medical radiotherapy devices and X-ray generating devices, and in some facilities such as accelerators and nuclear reactors (1–4). Lead is considered the basic material as a shield against ionizing radiation, but at the present time, studies tend to use materials that are less costly and environmentally friendly and have good efficiency as shielding materials that serve the community, whether they are flexible or non-flexible materials (5–7).

Among the recent studies in the field of shielding is the use of polymers as basic materials, such as polyethylene, polypropylene, polyester, and epoxy resins. Polymer materials have the characteristics of flexibility and ease of formation, which expands their use and susceptibility against

* **Corresponding author: Mohamed Elsafi,** Physics Department, Faculty of Science, Alexandria University, 21511 Alexandria, Egypt, e-mail: mohamedelsafi68@gmail.com
Wafa M. Al-Saleh: College of Science and Health Professions, King Saud Bin Abdulaziz University for Health Sciences, Hofuf, Al-Ahsa, P.O. Box 6664 Al-Ahsa, 31982, Saudi Arabia; King Abdullah International Medical Research Center, Hofuf, Al-Ahsa, Saudi Arabia
Mai R. H. Dahi: Physics Department, Faculty of Science, Alexandria University, 21511 Alexandria, Egypt
M. I. Sayyed: Department of Physics, Faculty of Science, Isra University, Amman, Jordan
Haifa M. Almutairi: Medical Physics Department, Umm Al-Qura University, Prince Sultan Bin Abdul-Aziz Road, Mecca, Saudi Arabia
I. H. Saleh: Department of Environmental Studies, Institute of Graduate Studies and Research, Alexandria University, Alexandria, Egypt

photons and neutrons (8–10). Polyester resin is relatively high-density polymer and therefore plays an important role in attenuating neutrons and photons. Yazdani-Darki et al. (8) investigated the radiation shielding properties of polyester with PbO nanoparticles. The authors found that the superior radiation attenuation sample is the sample with 60 wt% nanocomposite. Moradgholi and Mortazavi (9) studied the radiation shielding parameters for polyester doped with CdO. The authors reported an enhancement in the neutron attenuation due to the addition of CdO. The linear attenuation coefficient for the undoped sample was 0.187 cm^{-1}, and it decreased to 0.224 and 0.231 cm^{-1} due to the addition of 1% and 5% of CdO. Yulianti et al. (11), investigated a polyester composite reinforced by lead against X-rays photons. The authors found that as the lead content increased, the optical density increased, and X-ray transmission decreased. Hemily et al. (12) designed new marble composites based on polyester resins for use as protective shields from gamma radiation. The authors found that the samples with WO_3 nanoparticles have higher linear attenuation coefficient than the samples with micro WO_3. As reported by the authors, decreasing the particle size of WO_3 causes an improvement in the radiation shielding properties of the prepared samples. Sayyed et al. (13) studied the attenuation properties of polymeric materials, the matrix materials in the fabrication process were polyester resin and the fillers were some oxides such as B_2O_3 and TeO_2. The authors measured the radiation shielding factors using high purity germanium (HPGe) detector and different point sources. The linear attenuation coefficient (LAC) increased due to the addition of TeO_2, while the half value layer (HVL) decreased.

The waste is used in many applications, such as recycling, or added to some matrixes as auxiliary materials in the formation of the compound. From these waste iron filings (IFs), it is possible to grind IFs and add them as fine aggregate to concrete or mortar to improve its shielding and mechanical properties. One of the recent applications is the use of polymeric materials as basic materials to which quantities of IF waste are added (14–17). Satyaprakash et al. (18) studied the mechanical properties of concrete in case of sand replacement with filings and found that it improves compressive and tensile strengths.

In this study, the attenuation coefficients of photons and neutrons were determined for six polyester composites developed by adding different proportions of IF experimentally using narrow beam method and compared by XCOM software. This work introduces novel polyester composites doped with waste IF as radiation protection materials. The significance of this study lies in its contribution for developing eco-friendly, cheap, and non-toxic materials for use as radiation shielding materials.

2 Materials and methods

The matrix used in this work is polyester, which is one of the most important liquid polymers with good mechanical properties, ability to resist heat, and crystal transparency during use. Therefore, many industries depend on it, such as the manufacture of PET bottles, insulating films for wires, floors, and insulating surfaces, but in this work, polyester resins were used as matrix (19,20). The properties of the polyester resins used in this work are tabulated in Table 1.

In the blacksmithing, filings are produced as a result of cutting, scraping, and polishing raw iron materials. So, a quantity of fine IF was collected from a Blacksmithing factory in Egypt, then it was further ground and sieved with a 60 μm diameter sieve. The chemical compositions were tested using EDX analysis (21) as shown in Figure 1, while the shape and structure of the molecule were tested using SEM image (22) as shown in Figure 1. These IFs were added in different proportions to polyester to obtain compounds to be used as protective shields against radiation.

The composites were produced as 0%, 20%, 30%, 40%, 50%, and 60% waste IFs. Composites were coded as Poly (pure polyester), Poly-IF20 (80% polyester and 20% waste IF), Poly-IF30, Poly-IF40, Poly-IF50, and Poly-IF60. Table 2 shows the sample code, density, and weight compositions.

In the experimental measurements, a HPGe detector was used for attenuation coefficients determination at different gamma-ray energies emitted from ^{60}Co, ^{137}Cs, and ^{241}Am radioactive sources. The mechanism of measurements was graphed in Figure 2 (23–26).

The intensities in the absence and the presence of the Poly-IF composite (I_0 and$I$) can be calculated by the determination of the peak area using Genie-2000 software. From these intensities (at the same line energy), we can determine the LAC of Poly-IF sample of thickness (x) using Lambert–Beer expression as follows (27–29):

$$\mathrm{LAC} = \frac{-1}{x}\ln\frac{I}{I_0} \tag{1}$$

Table 1: Physical properties of the polyester resin

Properties	Values
Degree of saturation	8%
Melting point	249°C
Density	1.25 g·cm^{-3}
Compressive strength	140 MPa
Yield modulus	2–4 g·cm^{-3}
Tensile strength	55 MPa
Tensile elongation at break	2%

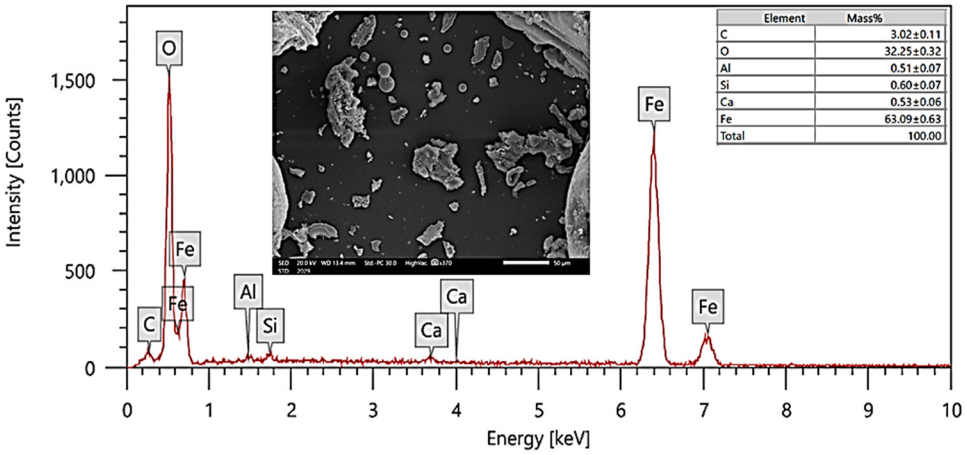

Figure 1: The morphological characteristics of waste IF.

Table 2: Compositions of fabricated polyester resin-IF samples

Code	Composition (wt%)		Density (g·cm^{-3})
	Polyester resin	IF	
Poly	100	0	1.252
Poly-IF20	80	20	1.572
Poly-IF30	70	30	1.747
Poly-IF40	60	40	1.965
Poly-IF50	50	50	2.246
Poly-IF60	40	60	2.620

XCOM is a widely used program to theoretically calculate gamma-ray attenuation coefficients, as well as interaction mechanisms for gamma-rays with an energy range from 1 keV to 100 GeV (30).

Attenuator coefficients such as mean free path (MFP), HVL, and tenth value layer (TVL) are calculated as an inverse function of the linear attenuation coefficient of the shield material as follows (31–33):

$$\text{MFP (cm)} = \frac{1}{\text{LAC}} \tag{2}$$

$$\text{HVL (cm)} = \frac{\ln(2)}{\text{LAC}} \tag{3}$$

$$\text{TVL (cm)} = \frac{\ln(10)}{\text{LAC}} \tag{4}$$

The radiation shielding efficiency (RSE) of Poly-IF composite which is used as a radiation shield is determined by using the initial (I_0) and transmitted (I) gamma line intensities obtained from peak area calculation (34).

$$\text{RSE (\%)} = \left[1 - \frac{I}{I_0}\right] \times 100 \tag{5}$$

The lead equivalent thickness (LE_{th}) corresponding to the Polyester–IF thicknesses used in this work was evaluated by the following formula (35):

$$\text{LE}_{\text{th}} = \frac{\text{LAC}_{\text{EP-IF}}}{\text{LAC}_{\text{Pb}}}. t_{\text{EP-IF}} \tag{6}$$

The possibility of a neutron passing through glass without interacting is described by the fast neutron removal cross-section (FNRC). Every composite's FNRC can be evaluated using (36)

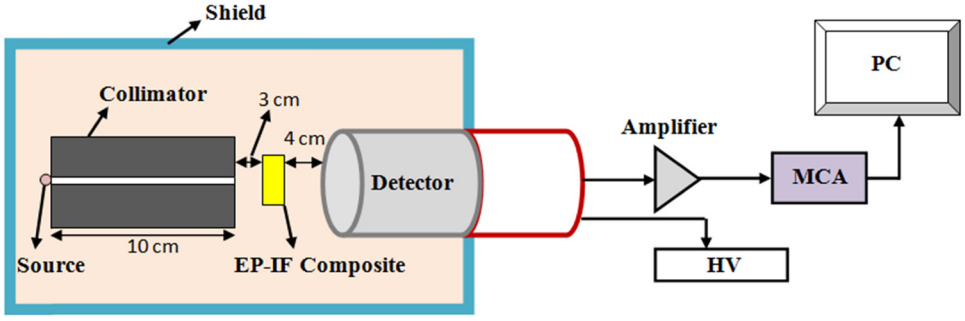

Figure 2: Schematic diagram of the experimental technique.

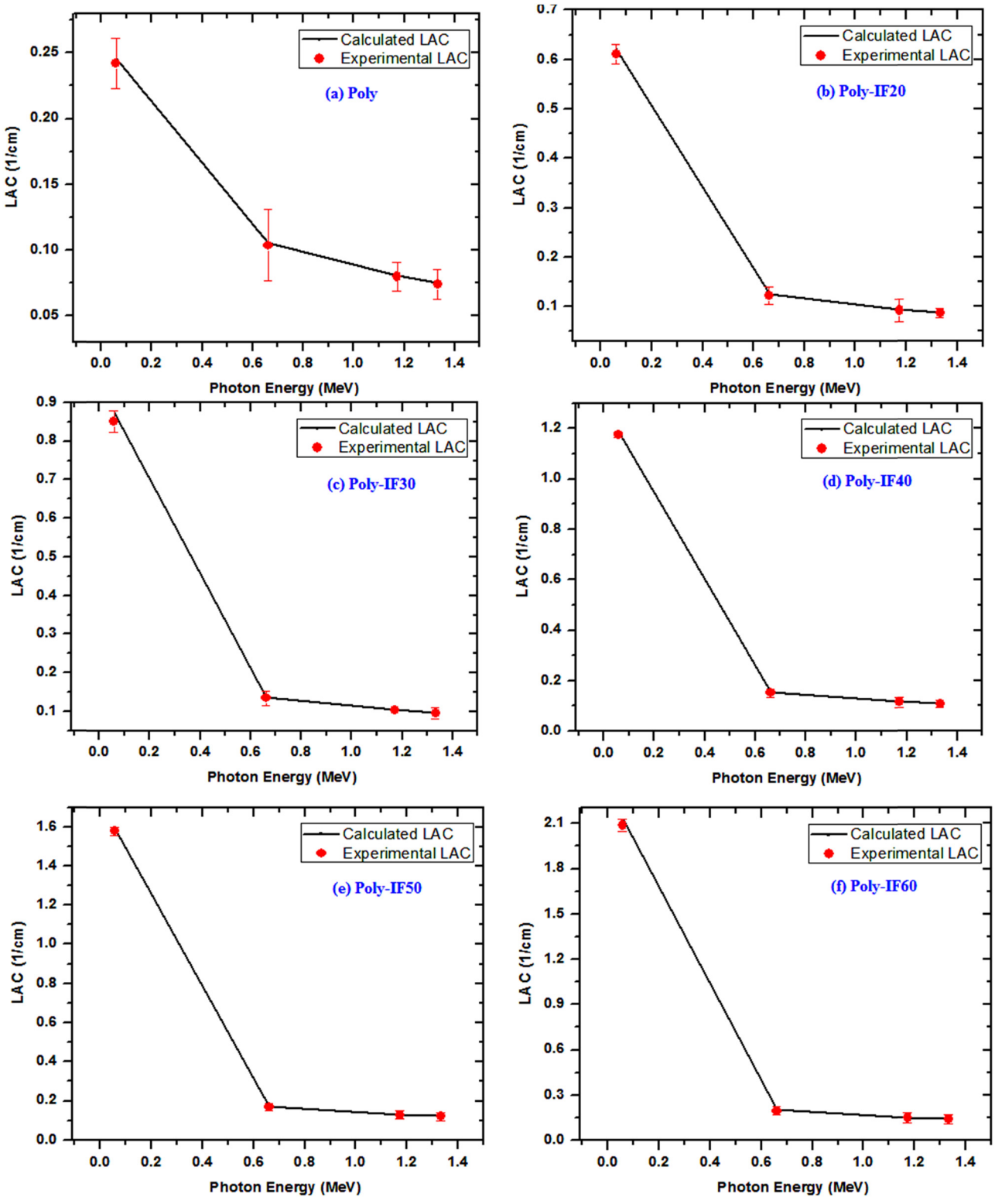

Figure 3: The calculated and experimental linear attenuation coefficient determined for the polyester samples: (a) Poly, (b) Poly-IF20, (c) Poly-IF30, (d) Poly-IF40, (e) Poly-IF50, and (f) Poly-IF60.

$$\text{FNRC} = \sum_i (\Sigma_R/\rho)_i w_i \quad (7)$$

where $(\Sigma_R/\rho)_i$ is the removal cross-section of the ith composite

3 Results and discussion

Figure 3 shows the calculated and experimental LAC determined for the polyester radiation shields at various photon energies. The aim of this figure is to ensure that the experimental LAC values closely align with the theoretical calculated values, so that further parameters which rely upon these results will also be accurate. Focusing on the pure polyester sample first, its theoretical LAC values range between 0.245 cm^{-1} at 0.060 MeV and 0.075 cm^{-1} at 1.333 MeV. Comparing these results (30) with the experimental values, a percent deviation between 0.91% and 2.13% is observed, which is well within the acceptable range for accurate determination of the shields' attenuation capability. Looking at some of the other samples, all the values remain in the same range. For example, Poly-IF30's percent deviation lies between 0.25% and 2.72%, while Poly-IF50's percent deviation lies between 0.72% and 2.16%. For all the samples at the four tested energies, the deviation never goes past 2.72%, which means that the experimental LAC values are very close to the theoretical ones and will accurately predict the overall shielding ability of the prepared polyester samples.

Figure 4 shows the LAC values of the polyester shields as a function of photon energy to compare the shielding ability of the materials against each other. The greatest difference between the LAC values of the samples occurs at 0.060 MeV, where the Poly-IF60 sample has a much greater LAC than the other shields, followed by the Poly-IF50 sample, Poly-IF40 sample, and so on until the pure polyester shield. This is due to the domination of photoelectric effect (37). Specifically, their values are equal to 0.245, 0.622, 0.873, 1.187, 1.591, and 2.129 cm^{-1} for Poly, Poly-IF20, Poly-IF30, Poly-IF40, Poly-IF50, and Poly-IF60, respectively. At 0.662 MeV and onward, however, the difference between the LAC values of the polyester shields is much smaller, but the same relative order is maintained. For example, the pure polyester sample's LAC is equal to 0.106, 0.081, and 0.075 cm^{-1} at 0.662, 1.173, and 1.333 MeV, respectively, while Poly-IF60's LAC is equal to 0.200, 0.151, and 0.142 cm^{-1} at the same respective energies. In other words, the Poly-IF60 sample has the greatest LAC at all energies, while the pure polyester sample has the least LAC. This means that the addition of IFs can improve the LAC and thus the radiation shielding properties of the prepared composites since iron has relatively high density.

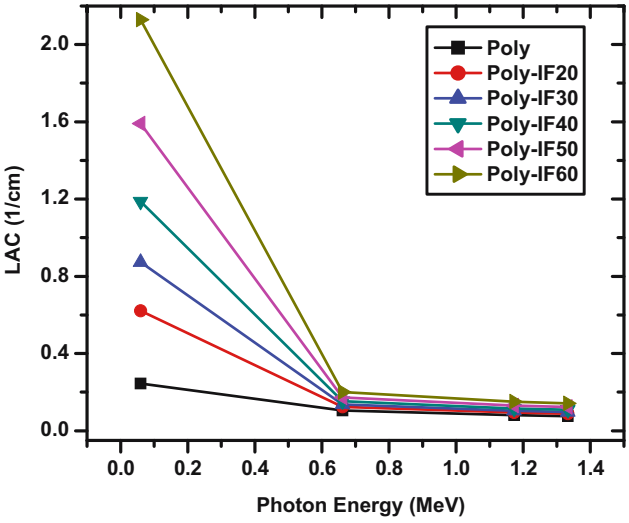

Figure 4: The linear attenuation coefficient determined for the polyester samples as a function of the energy.

Figure 5 shows the HVL, MFP, and TVL of the six tested samples against photon energy. Looking at all the parameters together, all three increase with the increase in the photon energy for all the samples (38). This suggests that the penetrating ability of the photons increases with the increase in the energy of the radiation. For example, Poly-IF20's HVL is equal to 1.114, 5.563, 7.320, and 7.816 cm at 0.060, 0.662, 1.173, and 1.333 MeV, respectively, while Poly-IF50's HVL is equal to 0.436, 4.003, 5.287, and 5.644 cm at the same energies. Meanwhile, their MFP values are equal to 1.607, 8.025, 10.561, and 11.276 cm for Poly-IF20 at the same respective energies and 0.629, 5.775, 7.628, and 8.142, respectively, for Poly-IF50. These upward trends occur because as higher energy photons gain more penetrating power, the sample's thickness must be increased to stop the same number of photons, and at the same time the distance between subsequent collisions, which is the definition of MFP, also increases (39). Focusing on only one parameter at a time, the values at any energy are inversely related to the quantity of IF in the sample. For instance, at 0.662 MeV, the TVL values are equal to 21.778, 18.479, 16.781, 15.058, 13.298, and 11.508 cm for Poly through Poly-IF60, respectively, while at 1.333 MeV they are 30.530, 25.963, 23.604, 21.205, 18.748, and 16.244 cm for the same respective samples. Thus, increasing the IF content in the samples lowers the HVL, MFP, and TVL of the shields, leading to greater shielding efficiency.

Figure 6 shows the transmission factor (TF) and radiation shielding efficiency (RSE) of the samples with a

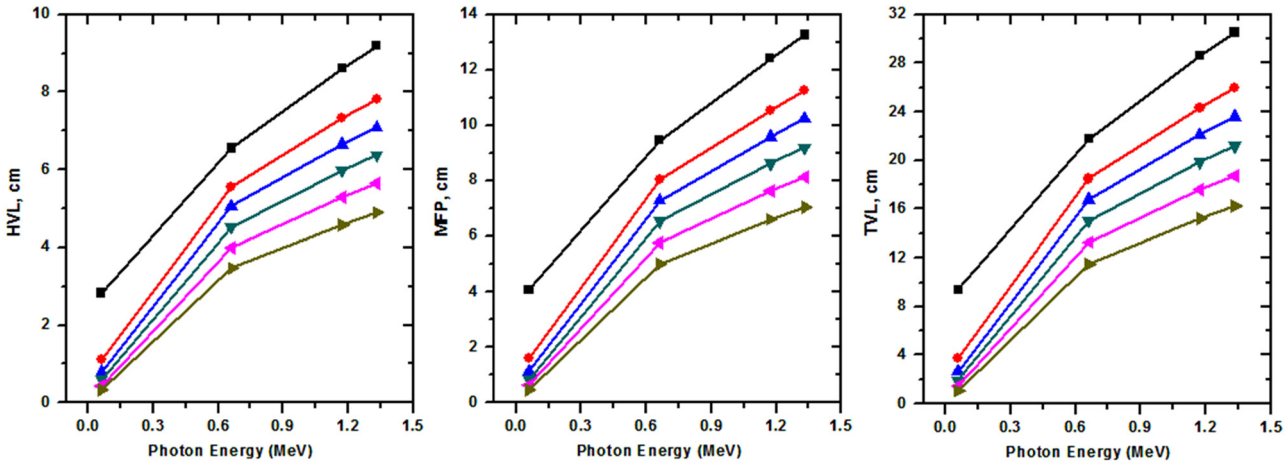

Figure 5: The HVL, MFP, and TVL for the prepared composites.

thickness of 2 cm at the four tested energies. The TF and RSE values show two opposite trends with energy, where the TF values increase with greater energy, while the RSE values drop when facing higher energy photons (40,41). For instance, Poly-IF30's TF is equal to 28.82%, 77.94%, 82.75%, and 83.75% at 0.060, 0.662, 1.173, and 1.333, respectively, while its RSE is equal to 82.57%, 24.00%, 18.80%, and 17.72%, respectively. Thus, higher energy photons can transmit or pass through the polyester samples easily than lower energy photons, or likewise the shielding efficiency of the materials drops when facing higher energy radiation. For this reason, we must increase the thickness of the shielding materials in order to block the high energy radiation (42). Furthermore, the TF values decrease at all energies when introducing more IFs to the polyester and the RSE values increase. For example, at 1.173 MeV, the TF values decrease from 85.12% to 82.75%, 81.20%, 79.31%, 76.94%, and 73.89% for Poly to Poly-IF60, respectively, while the RSE values increase from 14.88% to 17.25%, 18.80%, 20.69%, 23.06%, and 26.11% respectively. Therefore, it can again be concluded that the Poly-IF60 sample, the shield with the greatest IF concentration, has the most desirable attenuation capability.

Figure 7 shows the LE_{th} of the polyester samples as a function of the energy of the radiation. At the smallest tested energy, 0.060 MeV, the values are at their lowest, between 0.019 cm for Poly and 0.162 cm for Poly-IF60. As the photon energy increases, so does the LE_{th} for the

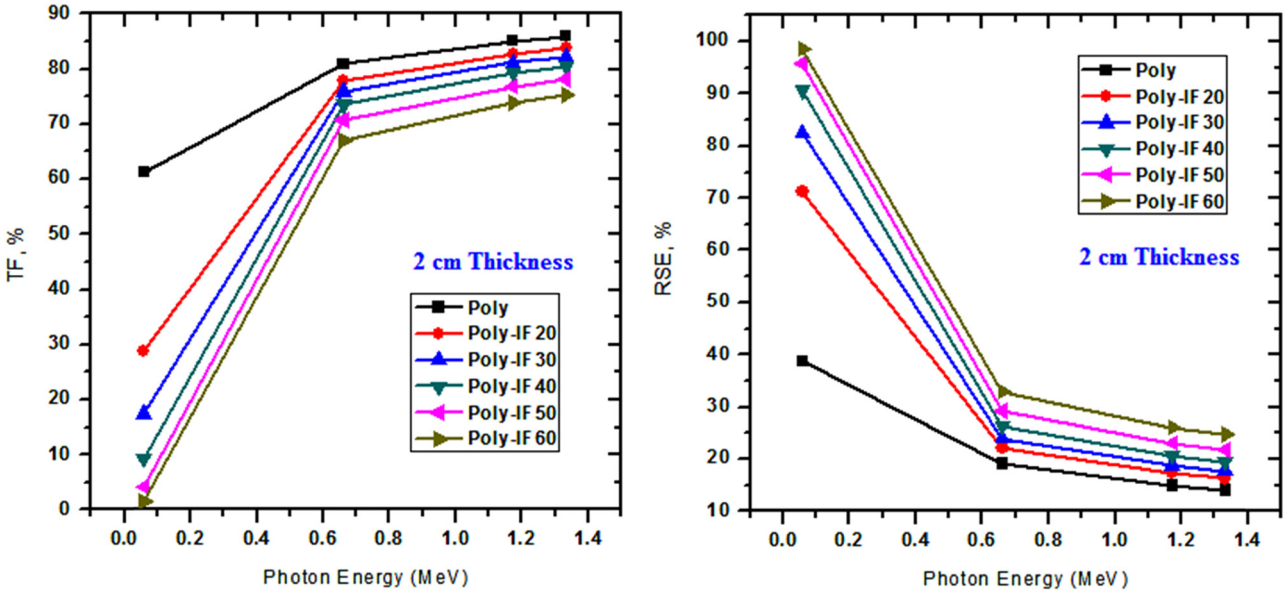

Figure 6: The TF and the RSE of the samples with a thickness of 2 cm.

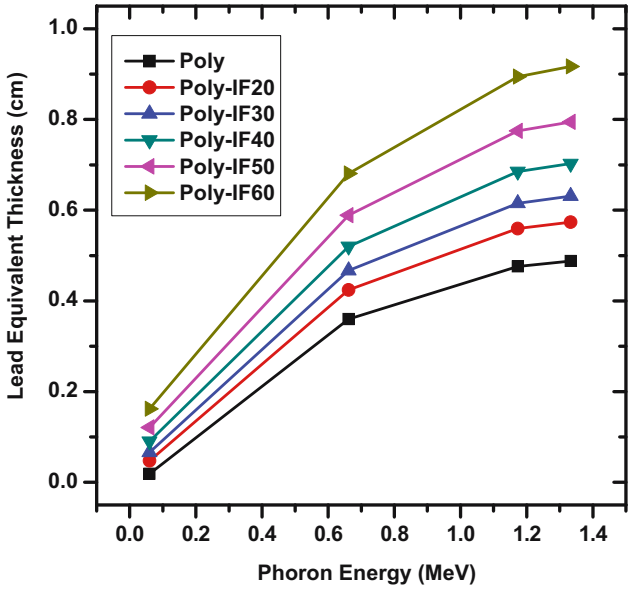

Figure 7: The LE_{th} of the polyester samples as a function of the energy of the radiation.

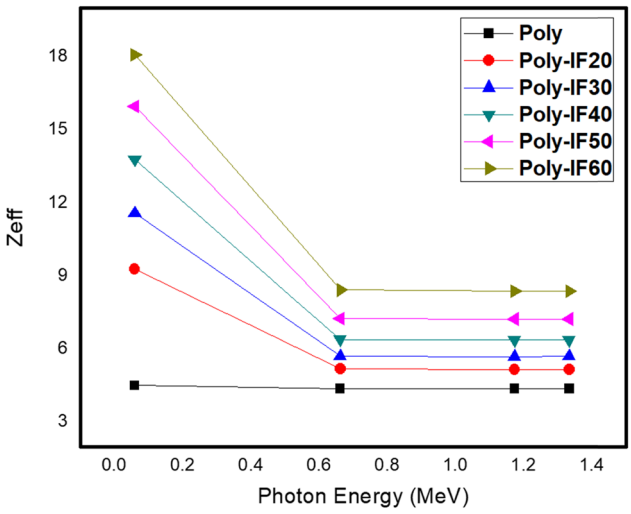

Figure 8: The Z_{eff} of the polyester samples as a function of the energy of the radiation.

samples. At 0.662 MeV, the values are between 0.360 and 0.681 cm for Poly and Poly-IF60, respectively, at 1.173 MeV they are between 0.476 and 0.894 cm, and at 1.333 MeV they are between 0.488 and 0.917 cm, respectively. Additionally, these values also show that the Poly sample has the lowest LE_{th} at all energies, while the Poly-IF60 sample has the greatest LE_{th} at all energies, following the order of the IF concentration in the samples. For example, at 0.662 MeV, the values are equal to 0.360, 0.424, 0.467, 0.520, 0.589, and 0.681 cm for Poly, Poly-IF20, Poly-IF30, Poly-IF40, Poly-IF50, and Poly-IF60, respectively, while at 1.333 MeV they are equal to 0.488, 0.574, 0.631, 0.702, 0.794, and 0.917 cm, respectively.

Figure 8 shows the effective atomic number (Z_{eff}) of the polyester samples as a function of the energy of the radiation. At 0.060 MeV, the Z_{eff} values are at their lowest, ranging from 4.52 for Poly to 18.08 cm for Poly-IF60. As the photon energy increases, the Z_{eff} decreases for all composites except for Poly, where the Z_{eff} for this sample is almost constant. The constant Z_{eff} for Poly can be explained according to the chemical composition of this sample, since it does not contain IF, and the atomic number of the consistent elements for this sample is close together, so we found that the Z_{eff} is almost constant (varied between 4.39 and 4.52). It is also clear from Figure 8 that the addition of IF causes an increase in the Z_{eff}. This is due to the increase in the proportion of the relatively high atomic number (i.e., Fe), so adding more IF to the prepared

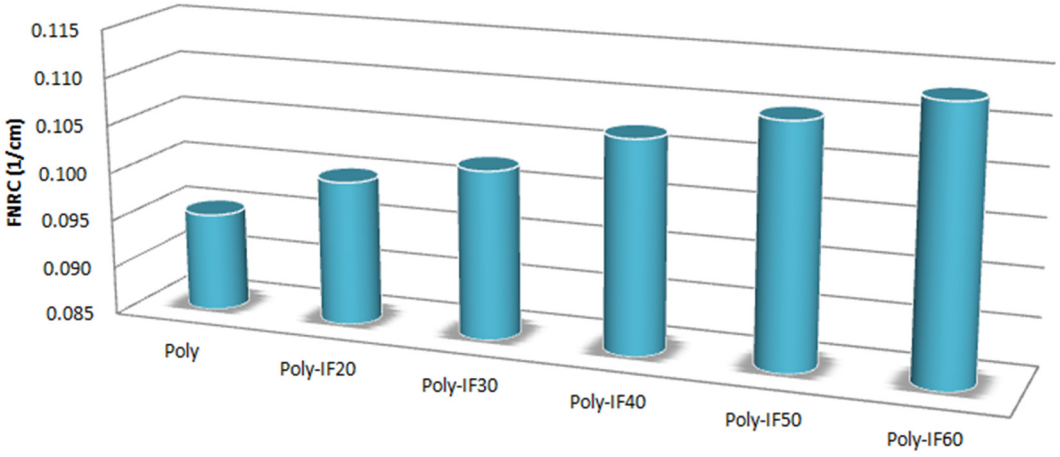

Figure 9: The FNRC of the polyester samples.

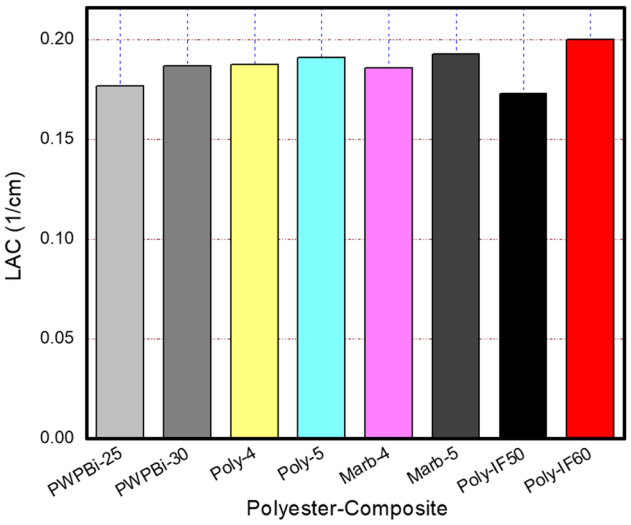

Figure 10: Comparison of present work with related published works.

composites lead to an increase in the Z_{eff}. For example, at 0.662 MeV, the Z_{eff} for the free IF composite (i.e., Poly) is 4.39, which increases to 8.43 for Poly-IF60, which means that the Z_{eff} is almost doubled. Also, at 1.173 MeV, the Z_{eff} is almost doubled due to the addition of 60% of IF, where the Z_{eff} increases from 4.39 (for Poly) to 8.39 (for Poly-IF60).

The FNRC of the polyester samples is graphed in Figure 9. The figure shows that the values of the samples increase when more Ifs are added to the samples. More specifically, the FNRC values are equal to 0.095, 0.100, 0.103, 0.107, 0.110, and 0.113 cm^{-1} for Poly, Poly-IF20, Poly-IF30, Poly-IF40, Poly-IF50, and Poly-IF60, respectively. Thus, the Poly-IF60 sample has the highest FNRC value, while the pure polyester sample has the lowest.

Finally, we compared the results of the highest LAC values with other related polyester-dependent composites (13,43,44) as shown in Figure 10. The results showed good efficiency against gamma rays for Poly-IF60 compared with other composites which indicated that it can be used as attenuators against incoming photons and neutrons.

4 Conclusion

Different polyester–IF composites were investigated for photons and neutrons shielding applications. The photon attenuation parameters were determined by experimental and theoretical methods such as LAC, MFP, and RSE. LAC determined for the polyester radiation shields at various photon energies (0.060, 0.662, 1.173, and 1.333 MeV). The greatest difference between the LAC values of the samples occurs at 0.060 MeV, where the Poly-IF60 sample has a much greater LAC than the other shields, followed by the Poly-IF50 sample, Poly-IF40 sample, and so on until the pure polyester shield. Specifically, their values are equal to 0.245, 0.622, 0.873, 1.187, 1.591, and 2.129 cm^{-1} for Poly, Poly-IF20, Poly-IF30, Poly-IF40, Poly-IF50, and Poly-IF60, respectively. The HVL, MFP, and TVL of the six tested samples against photon energy have been calculated. Looking at all the parameters together, all three increase with the increase in the photon energy for all the samples. The FNRC of the polyester samples was calculated and the values increase when more Ifs were added to the samples. More specifically, the FNRC values are equal to 0.095, 0.100, 0.103, 0.107, 0.110, and 0.113 cm^{-1} for Poly, Poly-IF20, Poly-IF30, Poly-IF40, Poly-IF50, and Poly-IF60, respectively. The outcome from this work opens up the opportunities for the improvement of the current radiation shielding materials and development of new materials for radiation protection with practical applications in different industries and medical facilities.

Funding information: The authors state no funding involved.

Author contributions: Wafa M. Al-Saleh: investigation, data curation, visualization, and funding acquisition; Mai R. H. Dahi: software, resources, and writing – original draft; M. I. Sayyed: investigation, data curation, and writing – review and editing; Haifa M. Almutairi: software, formal analysis, and visualization; I. H. Saleh: investigation, writing – original draft, and supervision; Mohamed Elsafi: conceptualization, methodology, and writing – review and editing. All authors have read and agreed to the published version of the manuscript.

Conflict of interest: The authors state no conflict of interest.

Data availability statement: All relevant data are provided within this article.

References

(1) More CV, Akman F, Dilsiz K, Ogul H, Pawar PP. Estimation of neutron and gamma-ray attenuation characteristics of some ferrites: Geant4, FLUKA and WinXCom studies. Appl Radiat Isotopes. 2023;197:110803, 0969-8043.

(2) More CV, Botewad SN, Akman F, Agar O, Pawar PP. UPR/Titanium dioxide nanocomposite: Preparation, characterization and application in photon/neutron shielding. Appl Radiat Isotopes. 2023;194:110688, 0969-8043.

(3) Kilicoglu O, More CV, Kara U, Davraz M. Investigation of the effect of cement type on nuclear shield performance of heavy concrete. Radiat Phys Chem. 2023;209:110954, 0969-806X.

(4) Elsafi M, Almuqrin AH, Yasmin S, Sayyed MI. The affinity of bentonite and WO_3 nanoparticles toward epoxy resin polymer for radiation shielding. e-Polymers. 2023;23(1):20230011. doi: 10.1515/epoly-2023-0011.
(5) Almuqrin AH, ALasali HJ, Sayyed MI, Mahmoud KG. Preparation and experimental estimation of radiation shielding properties of novel epoxy reinforced with Sb_2O_3 and PbO. e-Polymers. 2023;23(1):20230019. doi: 10.1515/epoly-2023-0019.
(6) Shahapurkar K, Gelaw M, Tirth V, Soudagar ME, Shahapurkar P, Mujtaba MA, et al. Comprehensive review on polymer composites as electromagnetic interference shielding materials. Polym Polym Compos. 2022;30:09673911221102127.
(7) Wu B, Zhu H, Yang Y, Huang J, Liu T, Kuang T, et al. Effect of different proportions of CNTs/Fe_3O_4 hybrid filler on the morphological, electrical and electromagnetic interference shielding properties of poly(lactic acid) nanocomposites. e-Polymers. 2023;23(1):20230006. doi: 10.1515/epoly-2023-0006
(8) Yazdani-Darki S, Eslami-Kalantari M, Feizi S, Zare H. Study of the structural and shielding properties of unsaturated polyester/lead oxide nanocomposites against gamma-rays. Radiat Phys Chem. 2023;209:110966.
(9) Moradgholi J, Mortazavi SM. Developing a radiation shield and investigating the mechanical properties of polyethylene-polyester/CdO bilayer composite. Ceram Int. 2022;48:5246–51.
(10) Liang S, Qin Y, Gao W, Wang M. A lightweight polyurethane-carbon microsphere composite foam for electromagnetic shielding. e-Polymers. 2022;22(1):223–33. doi: 10.1515/epoly-2022-0023.
(11) Yulianti I, Susanti T, Setiawan R. Lead-polyester resin composite as an alternative material for radiation protection in radiography. J Phys: Conf Ser. 2020;1567:032069.
(12) Hemily HM, Saleh IH, Ghataas ZF, Abdel-Halim AA, Hisam R, Shah AZ, et al. Radiation shielding enhancement of polyester adding artificial marble materials and WO_3 nanoparticles. Sustainability. 2022;14:13355. doi: 10.3390/su142013355.
(13) Sayyed MI, Yasmin S, Almousa N, Elsafi M. The Radiation Shielding Performance of Polyester with TeO_2 and B_2O_3. Processes. 2022;10:1725. doi: 10.3390/pr10091725.
(14) Alsaad AJ, Radhi MS, Taher MJ. Eco-friendly utilizing of iron filings in production reactive powder concrete. IOP Conf. Ser.: Mater. Sci. Eng. 2019;518:022051.
(15) Li R, Gu Y, Zhang G, Yang Z, Li M, Zhang Z. Radiation shielding property of structural polymer composite: Continuous basalt fiber reinforced epoxy matrix composite containing erbium oxide. Compos Sci Technol. 2017;143:67–74.
(16) Olutoge FA, Onugba MA, Ocholi A. Strength properties of concrete produced with iron filings as sand replacement. Curr J Appl Sci Technol. 2017;18(3):1–6. doi: 10.9734/BJAST/2016/29938.
(17) Miah MJ, Ali MK, Paul SC, John Babafemi A, Kong SY, Šavija B. Effect of recycled iron powder as fine aggregate on the mechanical, durability, and high temperature behavior of mortars. Materials. 2020;13:1168. doi: 10.3390/ma13051168.
(18) Satyaprakash, Helmand P, Saini. S. Mechanical properties of concrete in presence of iron filings as complete replacement of fine aggregates. Mater Today: Proc. 2019;15:536–45
(19) Madugu IA, Abdulwahab M, Aigbodion VS. Effect of iron fillings on the properties and microstructure of cast fiber–polyester/iron filings particulate composite. J Alloy Compd. 2009;476:807–11.
(20) Abushammala H, Mao J. Waste iron filings to improve the mechanical and electrical properties of glass fiber-reinforced epoxy (GFRE) composites. J Compos Sci. 2023;7:90. doi: 10.3390/jcs7030090.
(21) Rana S, Alagirusamy R, Joshi M. A review on carbon epoxy nanocomposites. J Reinf Plast Compos. 2009;28(4):461–87. doi: 10.1177/0731684407085417.
(22) Petrović JM, Bekrić D, Vujičić IT, Dimić I, Putić S. Characterization of glass-epoxy composites subjected to tensile testing. Acta Period Technol. 2013;151–62.
(23) Sayyed MI, Yasmin S, Almousa N, Elsafi M. Shielding properties of epoxy matrix composites reinforced with MgO micro- and nanoparticles. Materials (Basel). 2022 Sep 6;15(18):6201. doi: 10.3390/ma15186201, PMID: 36143510; PMCID: PMC9503172.
(24) Elsafi M, Almousa N, Almasoud FI, Almurayshid M, Alyahyawi AR, Sayyed MI. A novel epoxy resin-based composite with zirconium and boron oxides: An investigation of photon attenuation. Crystals. 2022;12:1370. doi: 10.3390/cryst12101370.
(25) Elsafi M, Almousa N, Al-Harbi N, Almutiri MN, Yasmin S, Sayyed MI. Ecofriendly and radiation shielding properties of newly developed epoxy with waste marble and WO_3 nanoparticles. J Mater Res Technol. 2023;22:269–77. doi: 10.1016/j.jmrt.2022.11.128.
(26) Sayyed MI, Hamad MK, Mhareb MH, Kurtulus R, Dwaikat N, Saleh M, et al. Assessment of radiation attenuation properties for novel alloys: An experimental approach. Radiat Phys Chem. 2022;200:110152.
(27) Almuqrin AH, Sayyed MI, Elsafi M, Khandaker MU. Comparison of radiation shielding ability of Bi_2O_3 micro and nanoparticles for radiation shields. Radiat Phys Chem. 2022;200:110170.
(28) Aloraini DA, Sayyed MI, Mahmoud KA, Almuqrin AA, Kumar A, Khandaker MU. Evaluation of radiation shielding characteristics of B_2O_3–K_2O–Li_2O - HMO (HMO = TeO_2/SrO/PbO/Bi_2O_3) glass system: A simulation study using MCNP5 code. Radiat Phys Chem. 2022;200:110172.
(29) Al-Harbi N, Sayyed MI, Al-Hadeethi Y, Kumar A, Elsafi M, Mahmoud KA, et al. A novel CaO–K_2O–Na_2O–P_2O_5 glass systems for radiation shielding applications. Radiat Phys Chem. 2021;188:109645.
(30) Gerward L, Guilbert N, Bjrn Jensen K, Levring H. X-ray absorption in matter. Reengineering XCOM. Radiat Phys Chem. 2001;60:23–4.
(31) Sayyed MI, Alrashedi MF, Almuqrin AH, Elsafi M. Recycling and optimizing waste lab glass with Bi_2O_3 nanoparticles to use as a transparent shield for photons. J Mater Res Technol. 2022;17:2073–83.
(32) Al-Hadeethi Y, Sayyed MI, Barasheed AZ, Ahmed M, Elsafi M. Preparation and radiation attenuation properties of ceramic ball clay enhanced with micro and nano ZnO particles. J Mater Res Technol. 2022;17:223–33.
(33) Hannachi E, Sayyed MI, Slimani Y, Elsafi M. Experimental investigation on the physical properties and radiation shielding efficiency of YBa_2Cu_3Oy/M@M_3O_4 (M = Co, Mn) ceramic composites. J Alloy Compd. 2022;904:164056.
(34) Hannachi E, Sayyed MI, Slimani Y, Almessiere MA, Baykal A, Elsafi M. Synthesis, characterization, and performance assessment of new composite ceramics towards radiation shielding applications. J Alloy Compd. 2022;899:163173.
(35) Al-Yousef HA, Alotiby M, Hanfi MY, Alotaibi BM, Mahmoud KA, Sayyed MI, et al. Effect of the Fe_2O_3 addition on the elastic and gammaray shielding features of bismuth sodium-borate glass system. J Mater Sci: Mater Electron. 2021;32:6942–54. doi: 10.1007/s10854-021-05400-z.
(36) Bashter II. Calculation of radiation attenuation coefficients for shielding concretes. Ann Nucl Energy. 1997;24:1389–401.

(37) Bilici S, Kamislioglu M, Guclu EEA. A Monte Carlo simulation study on the evaluation of radiation protection properties of spectacle lens materials. Eur Phys J Plus. 2023;138(1):80.
(38) Aygün B. High alloyed new stainless steel shielding material for gamma and fast neutron radiation. Nucl Eng Technol. 2020;52:647–53.
(39) Aygün B. Neutron and gamma radiation shielding Ni based new type super alloys development and production by Monte Carlo Simulation technique. Radiat Phys Chem. 2021;188:109630.
(40) Almuqrin AH, Sayyed MI, Elsafi M. A sustainable improvement of mortar by incorporation of marble dust and Zr_2O_3-NPs for radiation shielding applications. Radiat Phys Chem. 2023;212:111111.
(41) Azman MN Abualroos NJ, Yaacob KA, Zainon R. Feasibility of nanomaterial tungsten carbide as lead-free nanomaterial-based radiation shielding. Radiat Phys Chem. 2023;202:110492.
(42) Azman NZ, Jasmine JN, Almarri HM, Alshipli M, Ramzun MR. Radiation attenuation ability of bentonite clay enriched with egg-shell as recyclable waste for a physical radiation barrier. Radiat Phys Chem. 2022;201:110484.
(43) Almuqrin AH, Yasmin S, Abualsayed MI, Elsafi M. An experimental investigation into the radiation-shielding performance of newly developed polyester containing recycled waste marble and bismuth oxide. Appl Rheol. 2023;33(1):20220153. doi: 10.1515/arh-2022-0153.
(44) Sayyed MI, Almurayshid M, Almasoud FI, Alyahyawi AR, Yasmin S, Elsafi M. Developed a new radiation shielding absorber composed of waste marble, polyester, $PbCO_3$, and CdO to reduce waste marble considering environmental safety. Materials. 2022;15:8371. doi: 10.3390/ma15238371.